

Solid state synthesis and structural refinement of polycrystalline $\text{La}_x\text{Ca}_{1-x}\text{TiO}_3$ ceramic powder

O P SHRIVASTAVA*, NARENDRA KUMAR and I B SHARMA†

Department of Chemistry, Dr H S Gour University, Sagar 470 003, India

†Department of Chemistry, Jammu University, Jammu 180 006, India

MS received 17 November 2003; revised 13 January 2004

Abstract. Perovskite structure based ceramic precursors have a characteristic property of substitution in the “A” site of the ABO_3 structure. This makes them a potential material for nuclear waste management in synthetic rock (SYNROC) technology. In order to simulate the mechanism of rare earth fixation in perovskite, $\text{La}_x\text{Ca}_{1-x}\text{TiO}_3$ (where $x = 0.05$) has been synthesized through ceramic route by taking calculated quantities of oxides of Ca, Ti and La as starting materials. Solid state synthesis has been carried out by repeated pelletizing and sintering the finely powdered oxide mixture in a muffle furnace at 1050°C . The ceramic phase has been characterized by its powder diffraction pattern. Step analysis data has been used to determine the structure of solid solution of lanthanum substituted calcium titanate. The SEM and EDAX analyses also confirm that the CaTiO_3 can act as a host for lanthanum. X-ray data has been interpreted using CRYSFIRE and POWDERCELL softwares. The h, k, l values for different lattice planes have been generated from the experimental data. The lanthanum substituted perovskite crystallizes in orthorhombic symmetry with space group $Pnm\ a$ (#62). Following unit cell parameters have been calculated: $a = 5.410$, $b = 7.631$, $c = 5.382$. The calculated and observed values of corresponding intensities, 2θ , and density show good agreement. GSAS based calculation for bond distances Ti–O, Ca–O, La–O and bond angles Ti–O–Ca, Ca–O–Ca, La–O–Ti have been reported.

Keywords. Ceramic; La; Ca; titanate; GSAS; rietveld analysis; XRD; EDAX; SEM.

1. Introduction

The application of synthetic titanate and zirconate as host materials for fixation of nuclear waste in ‘synroc’ technology has been well established (IAEA 1977; Kesson 1983; Reeves and Ringwood 1983; Ringwood 1985; Ringwood and Kesson 1988). Leach rate experiments demonstrate that at temperatures above 100°C , titanate waste forms leached out hazardous cations at much slower rate than glass encapsulated wasteforms. The constituent synthetic minerals, viz. hollandite ($\text{BaAl}_2\text{Ti}_6\text{O}_{16}$), zirconolite ($\text{CaZrTi}_2\text{O}_7$) and perovskite (CaTiO_3), are reported to be kinetically stable in extreme geohydrothermal conditions (up to 900°C and 5000 bar) and are, therefore, more stable to leaching than borosilicate glasses (Cheary 1986; Kesson and White 1986; Cheary and Squadrito 1989; Gatehouse *et al* 1989). It has also been pointed out that the perovskite phase has a characteristic capability of converting several rare earths into titanate solid solutions at temperatures between 700°C and 1000°C . In this context it is desirable to understand the structure property relationship of rare earth substituted perovskites of $\text{M}_x\text{Ca}_{1-x}\text{TiO}_3$ compositions where M = rare earth (Goodenough *et al* 1976; Ringwood 1978; Myhra *et al* 1986). As a part of ongoing work, we have

reported the crystallochemical fixation of Sr in the perovskite structure wherein the strontium substituted perovskite crystallized in orthorhombic symmetry (Shrivastava and Shrivastava Rashmi 2002, 2003).

2. Experimental

To understand the crystallochemical interaction of calcium titanates with rare earths in nuclear waste forms, a simulation synthesis was carried out as follows: calculated quantities (molar ratio 0.05 : 0.95 : 1.0) of lanthanum, calcium and titanium were thoroughly mixed in glycerol medium using mortar and pestle. AR quality CaCO_3 , $\text{La}(\text{NO}_3)_3 \cdot 5\text{H}_2\text{O}$ and titanium oxide powder were used in appropriate quantities as source of Ca, La and Ti, respectively. The oxide route solid state synthesis of ceramic powder was carried out by repeated grinding, pelletizing and sintering the glycerol paste at 1050°C . After 72 h of sintering, densification of the material took place and a polycrystalline solid solution was formed. Powder X-ray diffractogram was recorded on a Rigaku multiflex diffractometer at the step size of 0.02° ($0.2^\circ/\text{min}$). All data points were recorded between $2\theta = 10$ and 70 . Scanning electron microscopic and EDAX analyses were performed to study the morphological characteristics and elemental analysis, respectively.

*Author for correspondence

3. Results and discussion

The preliminary powder diffractogram of the single phase polycrystalline perovskite ceramic powder of composi-

tion, $\text{La}_{0.05}\text{Ca}_{0.95}\text{TiO}_3$, gives about 20 prominent reflections between 10 and 70 (2θ) (figure 1). The reflections match in intensity and peak positions with the reported data on synthetic perovskite. The step analysis data

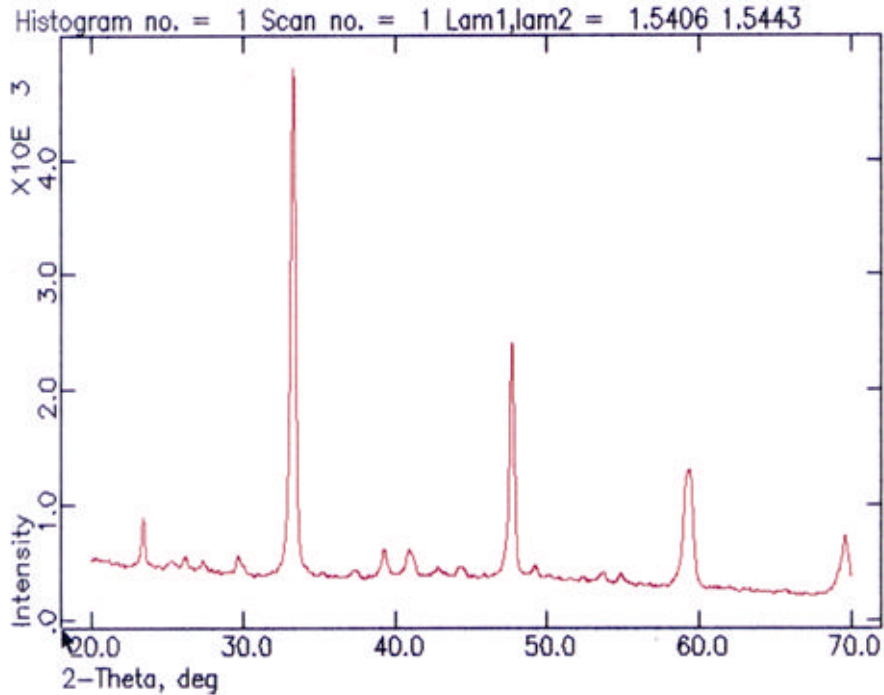


Figure 1. Observed X-ray diffractogram of $\text{La}_{0.05}\text{Ca}_{0.95}\text{TiO}_3$ ceramic powder.

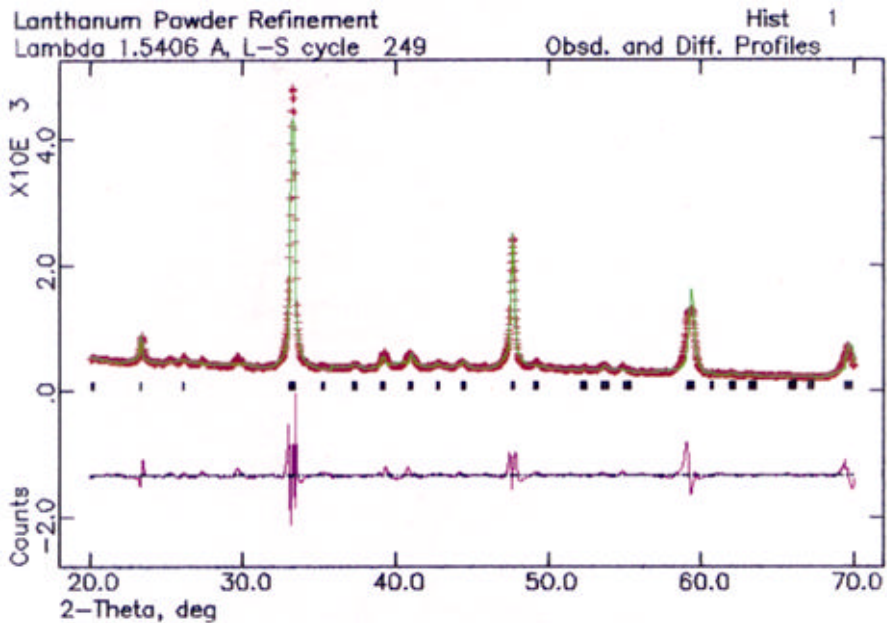


Figure 2. Rietveld refinement pattern of $\text{La}_{0.05}\text{Ca}_{0.95}\text{TiO}_3$. The '+' are the raw X-ray diffraction data, and the overlapping continuous line is the calculated pattern. Black vertical lines in the profile indicate the position of the allowed reflections for $\text{CuK}\alpha_1$ and $\text{CuK}\alpha_2$. The curve at the bottom is the difference in the observed and calculated intensities in the same scale.

consist of 2501 points between $2\theta = 20$ and 70° , where characteristic maxima is obtained at $2\theta = 33.00^\circ$. Out of these, 20 intense peaks were selected for indexing and calculation of unit cell parameters using CRYSFIRE software. The perovskite stoichiometry is expressed as ABO_3 where the size of the 'A' cation (divalent) is substantially large to form a close packed array with oxygen anion while the 'B' (tetravalent) ions must fit within the octahedral holes of the A–O close packed array. The ideal perovskite structure is cubic with $a = 3.8 \text{ \AA}$. The structure consists of B site cations that are octahedrally coordinated by atoms of oxygen. Larger A site cations are surrounded by twelve atoms of oxygen in cubo–octahedral coordination within this framework (Jacobson and Hutchinson 1980; Liu and Greedan 1994; Xianojun *et al* 2002). The reduction in symmetry from cubic to orthorhombic results from the presence in the A site of cations that are smaller than required to maintain the ideal geometry of this site. The calcium lanthanum titanate phase, $\text{Ca}_{1-x}\text{La}_x\text{TiO}_3$, present in nuclear wasteform has orthorhombic symmetry and the material crystallizes in the space group Pnm_a , the non standard setting of space group (#62). Rietveld analysis of the phase shows $R_{wp} = 11.84$ and $R_p = 7.65$ (figure 2) and the details of the crystal structure data and refinements are given in tables 1 and 2. Tables 3 and 4 list the bond lengths and bond angles and the Ca–O and Ti–O bond distances also match with the theoretical values of 3.20 and 1.93 \AA , respectively. Table 5 records indexed prominent reflections with their calculated and observed ' d '

Table 1. Crystal data for $\text{La}_{0.05}\text{Ca}_{0.95}\text{TiO}_3$ at room temperature.

Structure	Orthorhombic
Space group	Pnm_a
Point group	mmm
Symmetry of lattice	primitive
Lattice parameters	$a = b = c = 90$
	$a = 5.410$
	$b = 7.631$
	$c = 5.382$
R_{wp}	11.84
R_p	7.65
Volume of unit cell	222.189
Density _{cal}	4.213
Density _{exp}	4.20
Formula weight	563.674
χ^2	6.344
Slope	1.5352

Table 2. Final atomic coordinate of $\text{La}_{0.05}\text{Ca}_{0.95}\text{TiO}_3$ at room temperature.

Atom	x	y	z	Occupancy
O1	0.3170	0.5270	0.3260	1.00
O2	0.0180	0.2500	0.0370	1.00
Ca3	0.5300	0.2500	0.0110	0.95
La4	0.5300	0.2500	0.0110	0.05
Ti5	0.0000	0.0000	0.0000	1.00

values. The fourier map has been calculated by the program "forplot". It displays the single slice of the density map calculated by fourier in any orientation. This slice is produced by 8-point interpolation for each point in grid covering the slice area to the computed map and uses symmetry operations to complete the coverage (figure 3). The plots are square and contours depict the positions of titanium atoms in the title compound. The perovskite family of structures possess the capacity to accept a remarkably wide range of elements into solid solutions. Rare earths and trivalent actinides also preferentially replace calcium with charge neutralization being achieved by replacement of Ti^{4+} by Ti^{3+} , however, in presence of sodium a different mechanism is possible where rare earths may be incorporated as $\text{NaRETi}_2\text{O}_6$ which itself possess perovskite structure (Rivera *et al* 2002). Our findings on the ceramic phase, $\text{La}_{0.05}\text{Ca}_{0.95}\text{TiO}_3$, reveal that it crystallizes in orthorhombic symmetry but the mechanism of lanthanum substitution in the perovskite solid solution needs an explanation in terms of the charge compensation. Formation of cerium doped perovskite with no charge compensation has been reported elsewhere (Begg *et al* 1998). However, the

Table 3. Bond distances (\AA) and crystal coordinates of $\text{La}_{0.05}\text{Ca}_{0.95}\text{TiO}_3$.

		x	y	z
O1_Ca3	2.83885(0)	0.480	0.250	0.015
O1_Ca3	2.55647(0)	0.020	0.750	0.515
O1_Ca3	2.73539(0)	0.520	0.750	–0.015
O1_Ca3	2.92501(0)	–0.020	0.250	0.485
O1_La4	2.83885(0)	0.480	0.250	0.015
O1_La4	2.55647(0)	0.020	0.750	0.515
O1_La4	2.73539(0)	0.520	0.750	–0.015
O1_La4	2.92501(0)	–0.020	0.250	0.485
O1_Ti5	1.38079(0)	0.500	0.500	0.500
O1_Ti5	2.46331(0)	0.000	0.500	0.000
O1_Ti5	1.92009(0)	0.000	0.000	0.000
O1_Ti5	1.92209(0)	0.000	0.500	0.000

Table 4. Bond angles of $\text{La}_{0.05}\text{Ca}_{0.95}\text{TiO}_3$.

Angle	Degrees	atom1	loc	atom3	loc
Ca3_O1_Ca3	158.065(0)	1	000	2	000
Ca3_O1_La4	86.725(0)	1	000	–1	110
Ca3_O1_La4	158.065(0)	1	000	2	000
Ca3_O1_La4	86.725(0)	1	000	–1	110
Ca3_O1_Ti5	93.674(0)	1	000	2	000
Ca3_O1_La4	96.103(0)	2	000	–1	110
Ca3_O1_La4	0.000(0)	2	000	2	000
Ca3_O1_La4	96.103(0)	2	000	–1	110
Ca3_O1_Ti5	106.482(0)	2	000	2	000
La4_O1_La4	96.103(0)	–1	110	2	000
La4_O1_Ti5	104.942(0)	–1	110	2	000
La4_O1_La4	96.103(0)	2	000	–1	110
La4_O1_Ti5	106.482(0)	2	000	2	000
La4_O1_Ti5	104.942(0)	–1	110	2	000

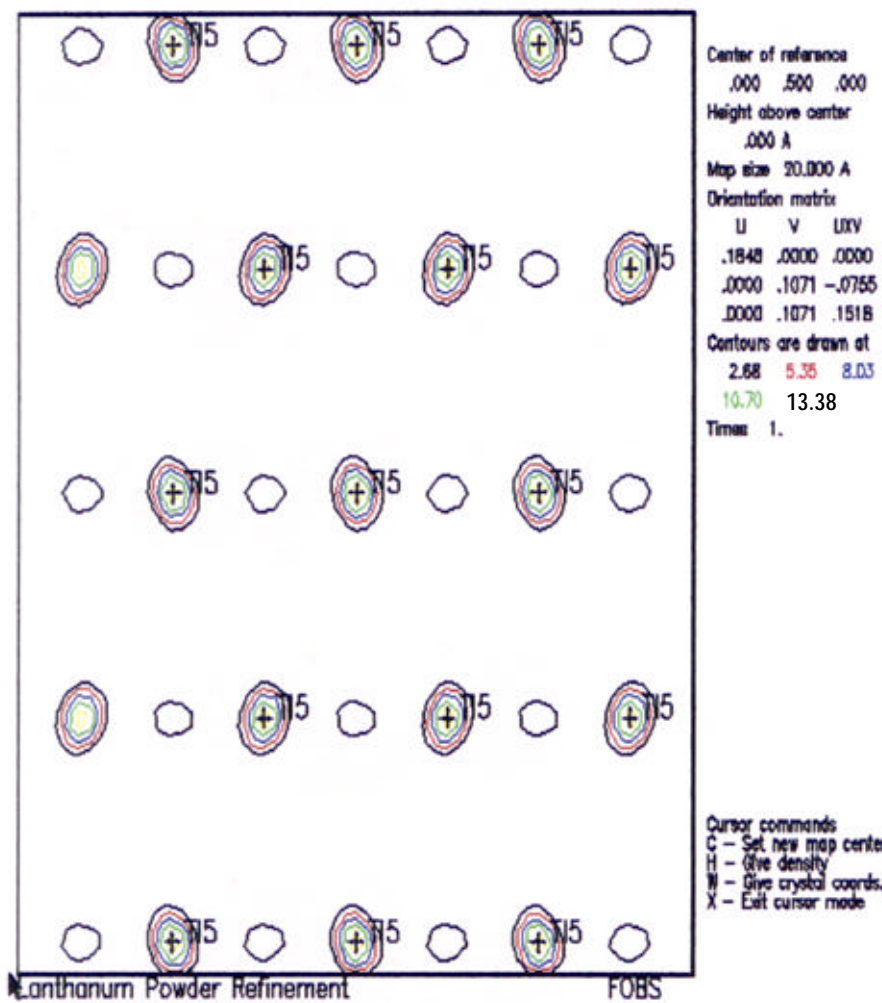


Figure 3. Calculated fourier map of $\text{La}_{0.05}\text{Ca}_{0.95}\text{TiO}_3$ ceramic powder.

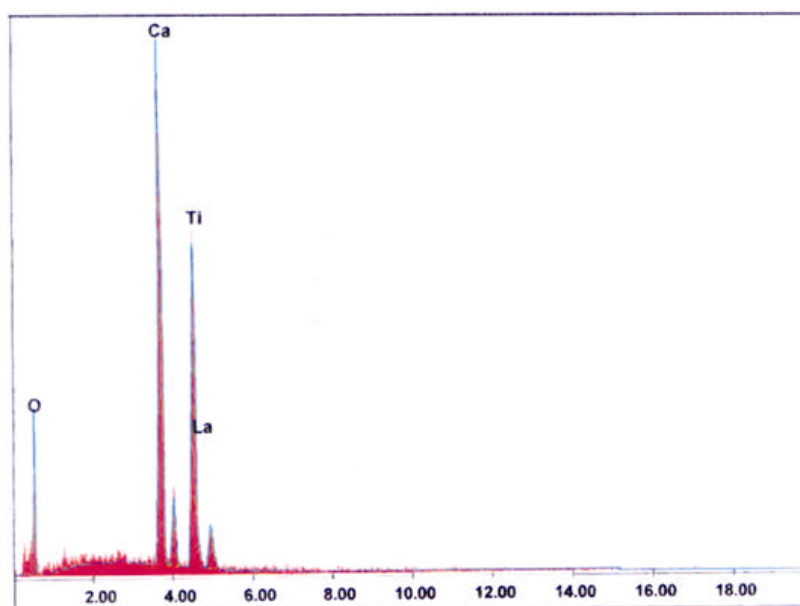


Figure 4. EDAX spectrum of $\text{La}_{0.05}\text{Ca}_{0.95}\text{TiO}_3$ ceramic powder.

Table 5. Indexed powder diffraction data of the lanthanum calcium titanate ceramic powder, $\text{La}_{0.05}\text{Ca}_{0.95}\text{TiO}_3$.

hkl	d_{obs}	d_{cal}	I_{obs}	I_{cal}
020	3.83	3.82	18.3	—
210	3.43	3.42	11.3	15.7
220	2.71	2.71	100.0	100.0
221	2.42	2.41	8.8	18.3
301	2.30	2.30	12.8	4.1
131	2.21	2.20	12.5	—
040	1.91	1.90	50.0	55.4
410	1.86	1.85	9.5	5.6
331	1.71	1.71	4.8	2.4
232	1.60	1.66	8.1	8.9
402	1.55	1.55	27.0	28.0
412	1.52	1.52	5.8	7.4
440	1.37	1.37	15.0	10.4
260	1.20	1.20	5.3	10.3
324	1.14	1.14	1.0	—

Table 6. EDAX analysis of the lanthanum calcium titanate ceramic powder.

Element	Weight (%)
La	4.42
Ca	30.23
Ti	30.72
O	34.63

charge compensation in reduced perovskite has been effected via trivalent titanium while cation vacancies offset the additional positive charge in air sintered perovskites. The perovskite's ability to self compensate in absence of specific charge compensating additives highlight their flexibility as hosts for multivalent waste ions such as lanthanides and actinides. Lanthanum ion can substitute for Ca^{2+} in perovskite (CaTiO_3) with the charge balanced by Ti^{4+} altering to Ti^{3+} in sites of TiO_6 octahedra surrounding the Ca^{2+} site (Szajman *et al* 1987). The alternate way of charge compensation through change in perovskite substoichiometry is also under investigation.

3.1 Scanning electron microscopy (SEM)

By scanning an electron probe across a specimen, high resolution images of the specimen with very high magnifications can be obtained. Compositional analysis of a material may also be obtained by monitoring secondary X-rays produced by the electron-specimen interaction. Thus detailed maps of elemental distribution can be produced from multi-phase materials. Characterization of fine particulate matter in terms of size, shape, and distribution as well as statistical analyses of these parameters have been performed. The scanning electron microscopy com-

**Figure 5.** Scanning electron microphotographs of $\text{La}_{0.05}\text{Ca}_{0.95}\text{TiO}_3$ ceramic powder.

pared with energy dispersive analysis used in the study of ceramics is generally of morphological interest. The weight% of Ca and La has been found to be 30.23 and 4.42, respectively in the samples of lanthanum calcium titanate precursors which correspond to the empirical formula on the basis of calculated quantities (table 6 and figures 4 and 5). The simulated ceramic waste form specimen consists of fine-grained crystals of size 0.05–1.5 μm . The size of a single crystal of synthetic perovskite is around $4.5 \times 1.5 \mu\text{m}$ with fine particles adhering to it.

Acknowledgements

The authors are thankful to the University Grants Commission, New Delhi, for funding the major research project No. F-12-137/2001(SR-I). We also thank Dr J P Shrivastava, Delhi University, Delhi, for his help in obtaining preliminary XRD data and Prof. T N Guru Row, IISc, Bangalore, for providing GSAS manual.

References

- Begg B D, Vance E R and Lumpkin G R 1998 *Mater. Res. Soc. Proc.* **506** 79
- Cheary R W 1986 *Acta Crystallogr.* **B42** 225
- Cheary R W and Squadrito R M 1989 *Acta Crystallogr.* **B45** 205
- Gatehouse B M, Grey R J, Hill and Rossel 1989 *Acta Crystallogr.* **B37** 205
- Goodenough J B, Hong H Y P and Kalfalas J A 1976 *J. Mater. Res. Bull.* **11** 203
- International Atomic Energy Agency Design and Operation of High Level Waste, Vitrification and Storage facility 1977 Technical report series no. 176, IAEA, Vienna
- Jacobson A J and Hutchinson J L 1980 *J. Solid State Chem.* **35** 334
- Kesson S E 1983 *Radioactive Waste Management Nucl Fuel Cycle* **4** 53
- Kesson S E and White T J 1986 *Proc. R. Soc. London* **A405** 73
- Liu G and Greedan J E 1994 *J. Solid State Chem.* **108** 371
- Myhra S, Giorgi R, Delogu P and Riviere J C 1986 *J. Mater. Sci.* **23** 1514
- Reeves K D and Ringwood A E 1983 *The synroc process for immobilization of high level nuclear waste, International conference on radioactive waste management IAEA-CN-43/127* (Seattle W.A.) (Vienna: IAEA) p. 16
- Ringwood A E 1978 *Safe disposal of high level nuclear reactor waste; A new strategy* (Canberra: Austral Nat Univ. Press) p. 64
- Ringwood A E 1985 *Min. Mag.* **49** 159
- Ringwood A E and Kesson S E 1988 *Radioactive waste forms for the future* (eds) W Lutzee and R C Erwing (Elsevier Sci. Pub. B.V.) p. 235
- Rivera A, Leon C, Santamaria J, Varez A, V'yunov O, Selous A G, Alonso J A and Sanz J 2002 *J. Chem. Mater.* **14** 5148
- Shrivastava O P and Shrivastava Rashmi 2002 *Prog. Cryst. Growth & Charact. Mater.* **45** 103
- Shrivastava O P and Shrivastava Rashmi 2003 *J. Indian Chem. Soc.* **80** 373
- Szajman J, Smart R.St.C. and Myhra S 1987 *Surf. Coat. Technol.* **30** 333
- Xianojun Kuang, Xiping Jing, Chun-K Loong, Eric E Lachowski, Skakle J M S and Anthony R West 2002 *Chem. Mater.* **14** 4359